공학석사학위논문

Multi-Core Liquid Crystal-Polymer Composite Fibers Produced by Electrospinning

전기방사를 이용한 다중코어 액정-고분자 섬유 제작

2015년 8월

서울대학교 대학원

융합과학부 나노융합전공

계 유 미

Abstract

Multi-Core Liquid Crystal-polymer composite Fibers Produced by Electrospinning

Yoo Mee Kye

Program in Nano Science and Technology

Department of Transdisciplinary Studies

Seoul National University

Electrostatic spinning, also known as electrospinning, is a technology which can produce long thin polymer fibers with diameter on the micro- or even nanoscales. In coaxial elecrospinning an additional capillary is introduced into the spinneret, allowing the inclusion of non-spinnable materials in the core of the fiber. As a result, the fiber may obtain new functionality provided by the core material. For instance, a low molar mass liquid crystal cannot be spun into fibers on its own, but it can be injected into a regular polymer fiber via coaxial elecrospinning. Such a liquid crystal-functionalized fiber acquires properties characteristic of liquid crystals, such as birefringence or selective reflection. The liquid crystal core can undergo phase transitions, allowing dynamic tuning of the properties and opening for applications in e.g. organic vapor detection.

In this research project, we grant more than one function to a single fiber by introducing two liquid crystals via dual-channel coaxial spinning. In our experiments, we use a glass capillary with theta-shaped cross section as spinneret as this provides a convenient way of introducing two separate capillaries for the two core materials. Stable dual core fibers could be produced provided that experimental factors such as flow rate, spinneret-collector distance, voltage, humidity and the characteristic of the collector are all optimized. We found that the stability of the dual-core structure as well as the shape of fiber strongly depends on whether the collector substrate is hydrophobic or hydrophilic. Samples were characterized by polarizing optical microscopy (POM) and scanning electron microscopy (SEM). The birefringence of the liquid crystal gives a unique color between crossed polarizers and it marks the inner channel structure of fiber. By heating we could determine whether or not the two core materials were well separated or if mixing had occurred. In case of well separated channels each core clears (transitions into an isotropic liquid) at a specific temperature which is different for the two cores. In contrast, if the two liquid crystals have mixed inside the fiber, then both cores become isotropic at one and the same temperature, which is intermediate between the clearing points of the individual materials. The cross section of fibers was monitored in detail through SEM.

In conclusion, we produced multichannel fibers functionalized with two different liquid crystals through coaxial elecrospinning. The characteristic of the liquid crystals revealed the inner channel system of fiber as well as its stability. This result shows that it is possible to produce multifunctional fibers via multi-channel coaxial electrospinning, but mixing of the different core materials is a critical problem which

can be difficult to avoid.

Keywords: Liquid crystal, Electrospinning, Functional fiber

Student Number: 2013-22393

Contents

Abstract ····· i

Contents ····· iv

List of Figures and Tables ····· vii

1. Motivation and Goal ····· **1**

2. Background ····· **3**

2.1 Liquid Crystals ····· 3

2.1.1 Nematics ····· 5

2.1.2 Cholesterics ····· 7

2.1.3 Alignment and Textures ····· 9

2.2 Electrospinning ····· 11

2.2.1 Fundamental Principle ····· 12

2.2.2 Coaxial Electrospinning ····· 13

2.2.3 Multiple-Core Coaxial Electrospinning ····· 15

2.2.4 Importance of Wettability of Collection Substrate ····· 16

3. Experiment ····· 17

3.1 Materials ····· 17

3.1.1 Polymers and Solvents ····· 17

3.1.2 Liquid Crystals ····· 19

3.1.3 Substrate Coating ····· 20

3.2 Electrospinning Set-up ····· 20

3.2.1 Atmosphere Control, Flow Control and Eclectic Field Application ····· 20

3.2.2 Spinneret Design ····· 23

3.2.3 Calculating Flow Rates ····· 26

3.2.4 Monitoring of Taylor Cone ····· 28

3.2.5 Polarizing Microscopy ····· 29

3.2.6 Scanning Electron Microscopy ····· 29

3.2.7 Electrospinning Conditions ····· 30

4. Results and Discussion ····· 31

4.1 Stable Spinning with Dual Core ····· 31

4.1.1 Monitoring of Tylor Cone and the onset of Spinning ····· 31

4.1.2 Counteracting Fiber Collapse after Collection in Target Substrate ····· 33

4.2 Two Cholesteric Liquid Crystals Encapsulated in the Same Fiber ····· 36

4.3 The Effect of Polymer Solution Concentration on the Inner Structure of the Fiber ····· 39

4.4 Dual Core Fiber with Two Different Encapsulated Namatic Liquid Crystals ····· 42

5. Conclusion ····· 51

6. Reference ····· 53

초록(국문) ····· 55

List of Figures and Tables

Figure 1 Nematic liquid crystal with director n. The angle between the director and the long axis of a single molecule is defined α and it is used in calculating the order parameter. ·····5

Figure 2 The trend of the thermotropic liquid crystal orientational order parameter as a function of temperature ·····6

Figure 3 Cholesteric liquid crystal with right handed helix structure. Blue arrows are the director of the liquid crystal and it rotates along the helix axis. ·····8

Figure 4 Selective reflection of chiral nematic liquid crystal. For further explanation, see main text. ····· 9

Figure 5 Sketch of dual core coaxial electrospinning set up. The inset shows the cross section of the composite spinneret, with the blue lines indicating the walls of the theta shaped glass capillary and the brown circles representing the silica capillaries that carry the two core materials·····15

Figure 6 Chemical structure of (a) polyvinylpyrrolidone and (b) titanium isopropoxide ····· 18

Figure 7 Chemical structure of surfactant (a) tetradecyltrimethylammonium bromide (14TAB) and (b) decyltrimethylammonium bromide (10TAB) ·····18

Figure 8 Chemical structure of liquid crystals. (a) E7, (b) 5CB and (c) CB15. ····· 19

Figure 9 Electrospinning chamber and tube with silica capillary which connected with vials ····· 21

Figure 10 First spinneret design with tube, silica capillaries, theta shaped glass capillary and syringe needle for voltage application ····· 23

Figure 11 Picture of second generation spinneret, designed with side branched connector and two metal needles guiding the core fluid capillaries (left) and the sketch of the spinneret (right)····· 25

Figure 12 Sketch of Taylor cone with ideal liquid flow (a) and in an unbalanced state (b). The imbalance of polymer solution and core fluid leads to the core material forming a drop within the Taylor cone. This can result in dripping or mixing of the two liquid crystals into a single core. A photograph of an ideally shaped Taylor cone with two nematic liquid crystal cores (one of them is doped with a black dye) is shown in (c)····· 32

Figure 13 Reflection state of polarizing optic image. The flow rate of polymer solution was 0.4 ml/hr and 0.96 ml/hr for each liquid crystal. The distance between the spinneret and collector was 13 cm while the applied voltage was 10.5 kV. The fibers were deposited on a glass slide. The scale bar is 20 μm.····· 34

Figure 14 Optical microscopy images of fibers with dye-doped ROTN in one core and chiral nematic in the other, in reflection (a), transmission (b) and reflection with crossed polarizer (c). The flow rate of polymer solution was 0.4 ml/hr and 0.96–1.1 ml/hr for liquid crystals. Distance between the spinneret and collector was 11.5cm while the supplied voltage was 7 kV. The sample is prepared on glass slide. The scale bar is 50 μm····· 35

Figure 15 Two different cholesteric liquid crystal core fibers. (a) had 0.4 ml/hr for polymer solution flow rate, 10cm distance and 6kV as supplied voltage while (b) had 0.8 ml/hr with 11.5cm distance and 7 kV. both of (a) and (b) had 4.8 ml/hr for liquid crystal flow rate····· 37

Figure 16 Heating experiment of fibers which were produced in a tapered glass capillary spinneret (340 μm diameter opening). The flow rate for polymer was 0.004 ml/hr while the core material had 0.77 ml/hr (67:33) and 1.94 ml/hr (50:50). The distance was 9cm with supplying 6kV voltage. The temperature is 20 ºC, 31 ºC, 33 ºC and 35 ºC in the sequence (a) to (d) ····· 38

Figure 17 Optical microscopy pictures of fibers produced with 16 wt% PVP. The image in (a) was obtained in reflection without polarizers, and that in (b) was in transmission with the sample between crossed polarizers. The flow rate for the polymer solution was 13.7 ml/hr and for the liquid crystals it was 0.4 ml/hr for 5CB and 1.29 ml/hr for the mixture of ROTN and CB15 (65:35 ratio). The distance from spinneret to collector was 13 cm and the applied voltage was 14.5 kV ····· 40

Figure 18 Fiber which produced with 20 wt% PVP. The picture (a) is the reflection with crossed polarization state, (b) is reflection without polarization and (c) is cross section sketch of dog bone shape fiber. The flow rate for polymer was 1.9 ml/hr and for liquid crystal were 0.04 ml/hr for E7 and 0.07 ml/hr for 5CB. Distance between the spinneret and collector was 6 cm and the supplied voltage is 8 kV····· 41

Figure 19 Fiber filled with E7 and 5CB observed in transmission between crossed polarizers. The fiber was prepared with flow rates: 0.8 ml/hr for polymer fluid, 0.13ml/hr for E7 and 0.09 ml/hr for 5CB. The temperature was 25 ºC, 40 ºC and 45 ºC from left to right····· 43

Figure 20 Cooled liquid crystal-filled fiber (same as in figure 19) after heating. Transmission state with polarizer (left) and reflection state (right) of the fiber ····· 44

Figure 21 5CB and E7 dual core fiber (red arrow) and mixed core fiber (blue arrow) deposited on hydrophobic substrate. The flow rate for polymer solution was 1.2 ml/hr and for liquid crystals were 0.07 ml/hr (5CB) and 0.05 ml/hr (E7). The distance between spinneret and collector was 8 cm and applied voltage was 10 kV ····· 45

Figure 22 The fibers from figure 21 as they are heated until all cores have gone through the phase transition to the isotropic state. The heating process was from 20 ºC to 46 ºC with a heating rate of 1 ºC/min. While the thick fiber with well separated dual cores shows two distinct clearing points at 25 ºC and 46 ºC, the thinner mixed core fiber has only one at 40 ºC.····· 46

Figure 23 Single liquid crystal fiber with 5CB (a–c) and E7 (d–f). While the bulk state of 5CB had phase transition at 33 ºC, the fiber prepared in the fiber had it at lower temperature, 28 ºC. E7 also experienced clearing point shift from about 60 ºC to 45 ºC····· 49

Figure 24 SEM images of cross section of a fractured dual core fiber spun with 5CB and E7, respectively, as core fluids, deposited on an OTS treated silicon substrate ····· 50

Table 1. Range of 5CB flow rate through the three types of flexible silica capillary used in the study, considering 25 cm capillary length ····· 27

Table 2. Cross section ratio for sheath solution and core material for each combination of our capillaries ····· 29

1 Motivation and Goal

In current studies, the interest for wearable technology is increasing. When people think about wearable technology, they typically consider small instruments with multiple functions which can be attached to a garment or worn on the body. In a longer term perspective, textiles which on their own are able to detect stimuli or exchange information can be the next form of wearable technology. In this sense, studies in functional textiles can help to expand the potential of wearable technology. The coaxial electrospinning technique is an appropriate method to produce functional composite fibers. These consist of a polymer sheath that encloses a core material of different composition. If the sheath is sufficiently thin and the polymer is appropriately selected, the characteristics of the core material can still be recognized in the composite fiber. The team of Dr. Jan Lagerwall succeeded in producing fibers with organic vapor sensor functionality, using liquid crystal as responsive core material. [1] The liquid crystal experiences a phase transition to an isotropic liquid state when the organic vapor enters through the sheath. This changes the optical appearance of the macroscopic fiber mat, allowing the detection of organic vapor with the naked eye.

Zhao and co-workers showed that it is possible to produce multi-core hollow fibers with coaxial electrospinning using multiple internal capillaries. [2] [3] [4] In this

thesis, we applied this concept to liquid crystal electrospinning with two different liquid crystals next to each other. We believe that the combination of two different responsive core materials will broaden the scope of functional textile application, for instance by incorporating cores responding differently to various gases, thereby allowing highly specific response. To reliably produce fibers with distinctly separated dual cores, we designed a new spinneret and deposited the fibers on substrates treated to be hydrophobic, and we optimized the conditions for electrospinning regarding concentration of polymer, flow rate, spinneret to collector distance and applied voltage. In this thesis, these procedures are described and explained step by step and examples of the resulting fibers are shown.

2 Background

2.1 Liquid Crystals

The term ‘phase’ indicates the state of matter at certain temperature and pressure. Crystalline solid, liquid and gas are the most common categories and these are distinguished based on the type and degree of ordering of the molecules. In crystalline solids the molecules are arranged with high degree of order in terms of position as well as orientation. In the liquid state, the ordering is short-range and the rotational and translational freedom of the molecules is larger. While the crystalline solid is hard due to tight restricted order, liquids are able to fluid and transforming their shape to fill the container.

In between the solid and liquid states, some materials exhibit one or several intermediate states, so called liquid crystal phases. The molecule ordering in liquid crystals is between that of crystals and ordinary liquids. They exhibit long range order and anisotropy, characteristics of crystalline solids, but also fluidity, the characteristic of liquids. Molecules that form liquid crystals are called mesogens. Their structure is characterized by the combination of rigid, often aromatic, sections and flexible aliphatic chains. While the rigid parts promote an ordered structure, the flexible ending

groups promote fluidity, granting characteristics of both crystal and liquid to the material. Mesogens are often organized according to the shape, the most common classes being rod-like (calamitic), disk-like (discotic) and banana-shaped (bent core). The phase of the liquid crystalline compounds discussed in this thesis depends on the temperature, giving them the category name thermotropic liquid crystals. In another class of liquid crystal, so called lyotropic liquid crystals, the concentration is the key variable. In addition to the melting point T_m, at which a thermotropic liquid crystal melts from the crystalline solid state, a liquid crystal also has a clearing point T_c where the liquid crystal transitions into the isotropic liquid state. [5]

Birefringence is another characteristic of liquid crystal, unique among liquids to exhibit this property. Birefringence, also called double refraction, is caused by the long range anisotropic structure of the material. When the light enters a birefringent material, it separates into two rays which experience different refractive indexes. The ray with polarization perpendicular to the optical axis passes though the material experiencing the *ordinary* refractive index (n_o) and we call this ray the *ordinary ray*. The other ray with polarization parallel to the optical axis experiences the *extraordinary* refractive index (n_e). This is consequently called the *extraordinary ray*. Because the two rays experience different refractive indexes, they pass through the material at different velocity and they have different wavelength within the material.

This characteristic leads to a phase shift between the components that may change the polarization. If a liquid crystal is placed between crossed polarizers, the sample often appears bright and colorful thanks to this effect. An isotropic material, in contrast, cannot change the polarization and it does appears dark in between the crossed polarizers.

2.1.1 Nematics

Nematic is the simplest liquid crystal phase with the least order. In a nematic liquid crystal the molecules arrange with uniform orientation over long distance. This common orientation is defined by a unit vector, the *director* **n**, as seen in **Figure 1**.

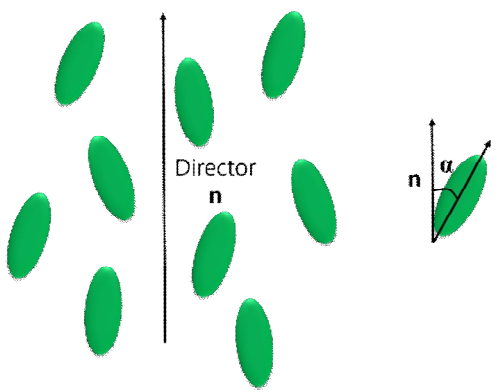

Figure 1. Nematic liquid crystal with director n. The angle between the director and the long axis of a single molecule is defined α and it is used in calculating the order parameter.

While the nematic phase exhibits long range orientational order, the positional order is

only short range. We can quantify this molecular ordering using the orientational order parameter, equation (1).

$$S = \frac{1}{2}\langle 3cos^2\alpha - 1\rangle \qquad (1)$$

The angle α in this equation is the angle between the director and the long axis of each molecule, and the pointed brackets indicate that we average over a probe volume. The order parameter of a liquid crystal is in the range between 0 and 1, where perfect orientational order would give S=1 while the isotropic liquid gives S=0. Thermotropic nematic liquid crystals have values around 0.3–0.4 at temperature close to the isotropic phase and higher values, 0.6–0.7, at lower temperatures, as sketched in **Figure 2**.

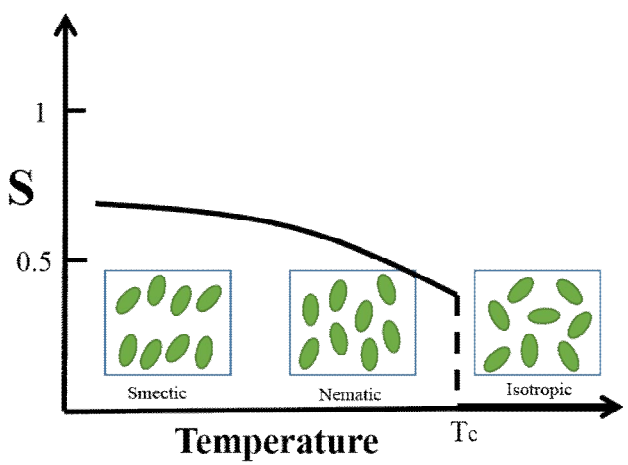

Figure 2. The trend of the thermotropic liquid crystal orientational order parameter as a function of temperature.

The smectic phases, of which SmA and SmC are the most important, exhibit one dimensional positional order in addition to the orientational order present in the nematic phase. In the smectic phases the molecule arrange in layers, that is, the one dimensional positional order is along the layer normal [6].

2.1.2 Cholesterics

While the ground state of the non-chiral nematic is characterized by a uniform director **n**, a chiral nematic prefers a helical modulation of the director. This chiral nematic is also called cholesteric. Locally, cholesteric liquid crystals have a nematic arrangement of the director **n**, but on a meso- to macroscopic scale **n** rotates along a helix oriented perpendicular to **n** as shown in **Figure 3**. The helical structure is induced by chiral mesogens or by added chiral dopant, which need not be mesogenic as long as it is miscible with the mesogens building the nematic phase. The latter method is called induced chiral system. The helix pitch, *p*, is the distance of one full turn of the director, and it typically ranges from about 0.1μm to several hundred μm. The inverse of the pitch indicates the strength of the chiral interactions. The helix can be right-handed or left-handed, depending on the molecules building up the phase. The cholesteric phase is abbreviated Ch or N*, where the latter abbreviation signifies that it is a chiral version

of nematic phase.

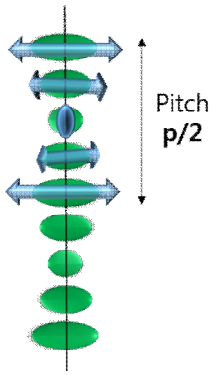

Figure 3. Cholesteric liquid crystal with right handed helix structure. Blue arrows are the director of the liquid crystal and it rotates along the helix axis.

If the pitch is on the order of a few hundred nanometers this helical structure brings a unique optical property named 'selective reflection' [7]. This phenomenon appears when the pitch matches the wavelength of visible light, and it is recognized by strong colors that can be observed with naked eye [5]. In detail, the reflection process is governed by Bragg's law, equation (2).

$$m\lambda = 2d \sin \theta \qquad (2)$$

The m in the equation is an integer and λ is wavelength of the incident wave inside of the material, d is the optical periodicity of the medium and θ is the incidence angle, as defined in **Figure 4** (a). Because **n** = **-n** (the director sign invariance) the optical properties of a cholesteric repeats with a distance of p/2, thus Bragg's law for

cholesterics takes the form:

$$m\lambda = 2\left(\frac{p}{2}\right)\sin\theta = p\sin\theta \qquad (3)$$

This explains the beautiful color of a cholesteric liquid crystal and how it changes depending on the pitch of the helix and on the angle of incidence (see **Figure 4** (b)).

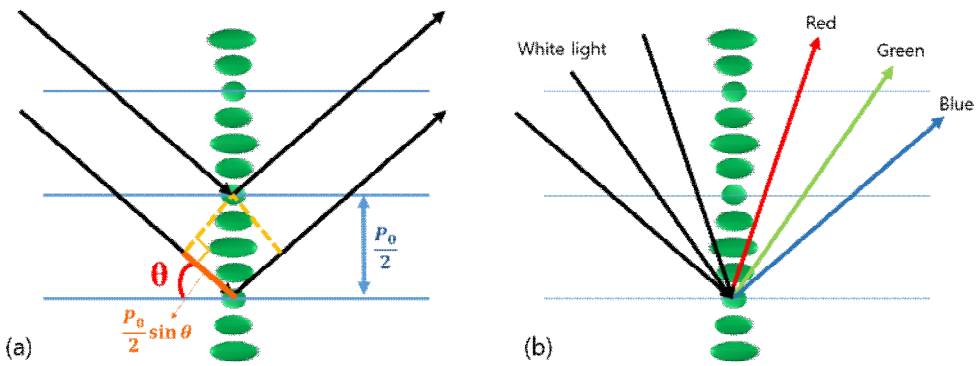

Figure 4. Selective reflection of chiral nematic liquid crystal. For further explanation, see main text.

2.1.3 Alignment and Textures

Liquid crystals are generally observed with polarizing microscopes, where the sample is placed between two crossed polarizers. The sample of liquid crystal is mostly prepared between two glass slides and the orientation of the liquid crystal can be controlled by preparing the slides which specific alignment agents. The two fundamental orientations are called planar and homeotropic, where the former means

that the director is in the plane of the sample, and the latter indicates a director that is perpendicular to the sample. Planar alignment is often induced by coating the glass slides with a thin layer of polymer, for instance, polyimide or nylon, which is rubbed unidirectionally in order to define the direction of **n**. If homeotropic alignment is desired, this can be achieved by coating the glass surface with a surfactant or other amphilic molecule. For instance, silanes such as octylsilane or octadecylsilane have a head group that makes a chemical bond with the glass substrate, directing the long alkyl chain perpendicular to the plane of the glass substrate. The silane chains guide the liquid crystal to have same perpendicular orientation.

A homeotropically aligned liquid crystal viewed in the polarizing microscope appears dark because the light propagation direction is along the optic axis, rendering all light ordinary (the light is polarized perpendicular to the optic axis). However, if we tilt the substrate along a direction between the two polarizers the sample appears bright since we then have both ordinary and extraordinary rays, giving rise to a change of polarization due to birefringence. This allows us to distinguish a homeotropic sample from an isotropic sample.

A planar-aligned liquid crystal can also appear dark if the director is along the polarizer or the analyzer. This is because for these two alignments we have only ordinary or only extraordinary light, respectively, and birefringence requires both

components. If, on the other hand, the director is oriented between the two polarizers birefringence is active and the sample appears bright in the polarizing microscope. In case of non-uniform planar alignment, i.e. the director is in the plane of the sample but the orientation in this plane varies, some areas may appear bright, others dark.

2.2 Electrospinning

Electrospinning has been researched in material science as a means to produce composite, sometimes smart, fibers. Among the advantages are comparatively low costs for the setup, small scale and a one-step spinning process, giving easy access for scientists to study the fiber formation. Various materials have been used in electrospinning to give different functions to fibers. Moreover, by controlling certain factors of the experiment, the fiber diameter can be tuned from tens of micrometers down to about hundred nanometers, the morphology can be varied from smooth to porous [8], and the fibers can be made hollow [9] or with different material in the core [10] [11]. The so called coaxial electrospinning modification allows the incorporation of low-molar mass liquids inside the fiber, thereby opening new potential for functional fibers. For instance, the combination of liquid metal core with an electroluminescent ionic transition metal complex mixed into the sheath polymer, finally with evaporated

coating of indium tin oxide, allowed a fabrication of LED fibers [12].

2.2.1 Fundamental Principle

The basic set up of electrsospinning consists of three parts - spinneret, collector and high voltage power supply. A polymer solution or melt is pumped to the spinneret at constant rate. The power supply is connected between spinneret and collector (grounded) and gives high voltage from 1 to 30 kV between them. Without the voltage, the polymer solution emerges from the spinneret, forming a droplet that grows in size until it detaches by its own weight. The surface tension promotes a (hemi-) spherical shape of the droplet. When the high voltage is applied, ions present in the solution are separated, one species drawn to the spinneret, the other pushed away from it toward the bottom of the droplet. The electrostatic forces on the latter distorts the droplet from the original hemispherical to a more or less cone shaped protrusion. This is called the Taylor cone after the first person who studied this phenomenon, Sir Geoffrey Ingram Taylor. Eventually, as the voltage is continuously increased, these forces overpower the surface tension and a thin jet is ejected from the bottom of the droplet [13].

During the flight from spinneret to collector, the jet fluid experiences considerable stretching due to the repulsion between equally charged ions, leading to a

rapidly increasing surface area. This in turn speeds up the evaporation of the solvent used (in case of melt electrospinning there is no evaporation of solvent). A few centimeters away from the spinneret, the straight jet becomes unstable and it undergoes a spiral-like distortion referred to as a 'whipping' process. This further reduces the thickness of the fiber, eventually reaching diameters as thin as about hundred nanometers under appropriate conditions. Finally, the solidified fibers are collected on the collector or on a substrate held into the jet. [14].

The produced fibers can be controlled in terms of their morphology by tuning the conditions of electrospinning. Environment factors such as humidity and temperature, set-up factors like distance between the spinneret and collector, the applied voltage, and the diameter of the spinneret are examples of the controllable factors. Also the details of the polymer solution and its flow, for instance concentration, viscosity, polymer molar mass, conductivity and flow rate, are important for the results.

2.2.2 Coaxial Electrospinning

Coaxial electrospinning is a modification that allows the introduction of new material in the fiber core. One or more inner capillaries are introduced into the main spinneret, through which the polymer solution for the sheath is flowing, giving us the possibility

to include different core materials. **Figure 5** shows a schematic for a dual core coaxial electrospinning configuration, as was used for the work described in this thesis. During the spinning, the outer polymer solution fluid encapsulates the core material, eventually leading to core-shell structured fibers. While the outer solution must contain a polymer of high molar mass at sufficient concentration in order to counteract the Rayleigh instability (which breaks up low molar mass fluid jets into droplets as the result of surface tension), the requirements on the inner fluid are much less restrictive. This means that also materials that normally are considered non-spinnable can be used as core solution, such as alkanes [15] or mineral oil [9]. This core-shell fiber is able to not only store the core material, but also let the core material sustain its characteristics in the fiber. For instance, a short pitch cholesteric liquid crystal can render the fiber colorful as a result of its selective reflection [16]. As another example, a random aligned network of fibers with non-chiral nematic core can be used to detect organic vapors, thanks to the change in optical properties when the vapor diffuses into the core and turns the liquid crystal isotropic. [1]

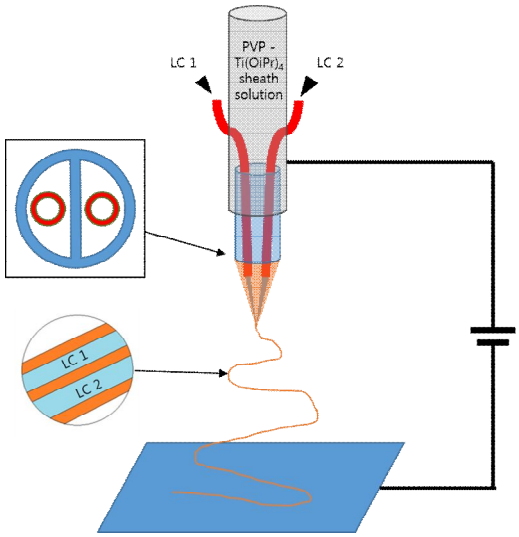

Figure 5. Sketch of dual core coaxial electrospinning set up. The inset shows the cross section of the composite spinneret, with the blue lines indicating the walls of the theta shaped glass capillary and the brown circles representing the silica capillaries that carry the two core materials.

2.2.3 Multiple-Core Coaxial Electrospinning

The advantage of spinning fibers with multiple cores, achieved by inserting more than one capillary in a coaxial electrospinning set-up, is that one and the same fiber can be given more than one functionality. For instance, a dual core fiber with two different alkanes in the cores showed an increased range of temperature insulation thanks to the different melting points of the two core materials [3]. If the core materials are removed after spinning, a low weight fiber with multiple hollow channels results, exhibiting

good insulation property. [2]

2.2.4 Importance of Wettability of Collection Substrate

In a recent study of the morphology of coaxial electrospun fibers, Dae Kyom Kim and Jan Lagerwall demonstrated that the surface property of the substrate on which fibers are collected may strongly affect the final fiber characteristics [17]. By imaging thin sections of the fibers, prepared by focused ion beam (FIB) lift-out, with high resolution transmission electron microscopy (HR-TEM), they found considerable differences between fibers collected on hydrophilic and hydrophobic substrates, respectively. In the former case, the fibers were strongly collapsed much core material had escaped. They explained these observations by considering the water condensating on the fiber during spinning, due to cooling as the solvent evaporates. On a hydrophilic substrate this can give rise to strong capillary forces as the water spreads on the substrate, leading to deformation of the fiber and the loss of core material. On hydrophobic substrate, in contrast, the water cannot spread and the impact on the final fiber quality is much less. As we will see in the following, the same phenomenon can have drastic implications for dual core coaxial fibers.

3 Experimental

3.1 Materials

3.1.1 Polymers and Solvents

Solutions of polyvinylpyrrolidone (PVP, see **Figure 6**) of molar mass 1.3 Mg/mole in anhydrous ethanol were prepared at concentrations varying from 15wt% to 20wt%. Solutions containing 5ml ethanol were stirred overnight in order to fully dissolve the polymer. In most of the experiments titanium isopropoxide ($Ti(OiPr)_4$, see **Figure 6**) was added as well as acetic acid. The latter is a catalyst for the hydrolysis of the former when the solution comes into contact with water that condensates from air during spinning. In using $Ti(OiPr)_4$, the dehydrated ethanol is very important because of the chemical reaction between the water and $Ti(OiPr)_4$. When the $Ti(OiPr)_4$ meet the water, it rapidly react and forms insoluble white power, $Ti(OH)_4$ [18] while the adding acetic acid help in forming Ti-O-Ti bridges [19]. Compare to the solvent which prepared with absolute ethanol, the polymer solution with some water included is less transparent and have yellow white dull color. Additionally, it easily produce the flat ribbon shape fibers. This turns the $Ti(OiPr)_4$ into TiO_2, giving the fibers a composite sheath of TiO_2 nanoparticles in a PVP matrix, generally leading to better fiber stability and more

cylindrical shape and promoting a stable coaxial jet [9] [15]. The volumes of $Ti(OiPr)_4$ and acetic acid were 0.15 ml and 0.1 ml, respectively. Finally, 0.02 mg of a cationic surfactant, tetradecyltrimethylammonium bromide (14TAB) or decyltrimethylammonium bromide (10TAB) (see**Figure 7**), is added for increasing the electrical conductivity and decreasing the surface tension of the polymer solution.

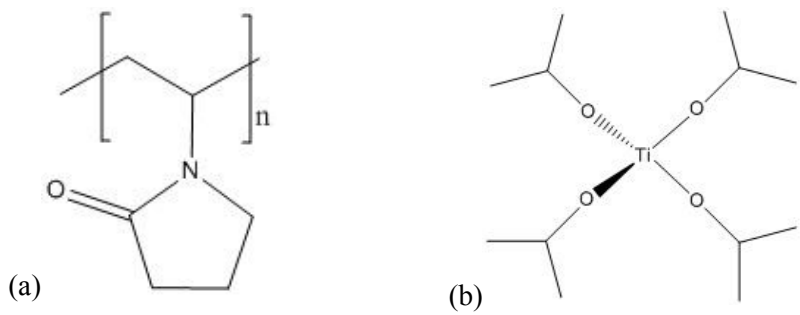

(a) (b)

Figure 6. Chemical structure of (a) polyvinylpyrrolidone and (b) titanium isopropoxide

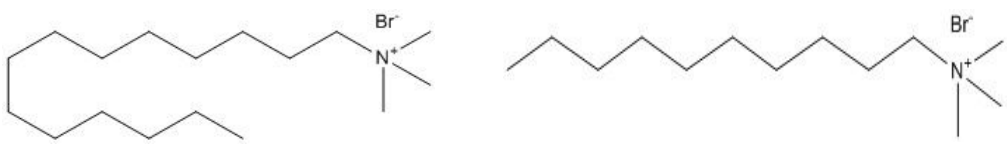

(a) (b)

Figure 7. Chemical structure of surfactant (a) tetradecyltrimethylammonium bromide (14TAB) and (b) decyltrimethylammonium bromide (10TAB)

3.1.2 Liquid Crystals

As non-chiral nematic liquid crystal, 5CB and E7 (see **Figure 8**) were used. These two liquid crystals were chosen because they have more than 20 ºC difference in clearing point, making it easy to distinguish them in heating experiment. Additionally, we used the commercial mixture ROTN 615, which is a broad temperature range nematic mixture with small amount (0.5 wt%) of chiral dopant, in one case mixed with a small amount of black dye (exact concentration is unknown) and in another case mixed with the chiral dopant CB15 (see **Figure 8**), in order to induce cholesteric liquid crystals with visible selective reflection. The amount of chiral dopant decides the pitch of the cholesteric helix, thus the color reflected by the liquid crystal. The higher the ratio of CB15 to ROTN 615, the shorter the pitch. With a mixture ratio 35:65 we get red reflection while a 50:50 ratio leads to blue color.

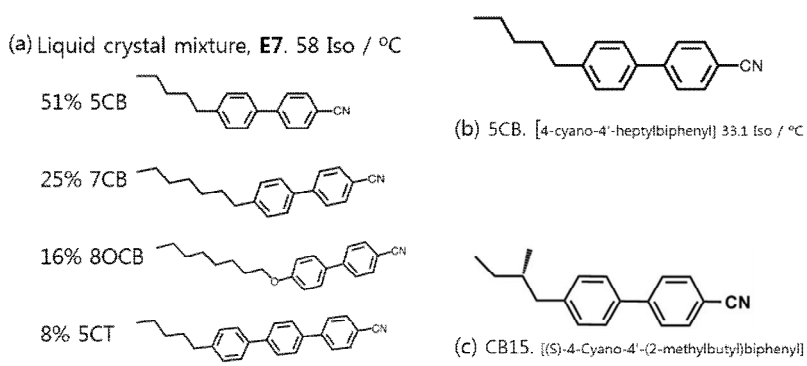

Figure 8. Chemical structure of liquid crystals. (a) E7, (b) 5CB and (c) CB15.

3.1.3 Substrate Coating

As mentioned above, the surface characteristics of the collection substrate can have considerable effect on the fiber morphology. Hydrophobic substrates are preferable because they prevent the flattening of fibers due to capillary forces from condensated water after fiber deposition. Therefore, silicon wafers were prepared with a monolayer coating of octadecyltricholorosilane (OTS). The OTS treatment was done either with vapor deposition [20] or solution immersion method [21].

3.2 Electrospinning Set-up

3.2.1 Atmosphere Control, Flow Control and Electric Field Application

To minimize the impact of environment factors such as inappropriate temperature or high humidity, the electrospinning experiment was carried out in a transparent acryl chamber with 40 cm by 40 cm cross section and 36 cm height, shown in **Figure 9**. The humidity is a particularly important factor which can greatly impact the morphology and diameter of fibers. [22] [23] Therefore, dry air was led into the main compartment of the spinning chamber. The upper level of the chamber was designed to store the

vials for the spinning fluids and to fix the spinneret into the ceiling of the main compartment. This compartment had a height of 26 cm, giving a maximum possible distance between the spinneret and collector of 25 cm. Smaller distances were easily achieved by placing the collector on an adjustable lab jack.

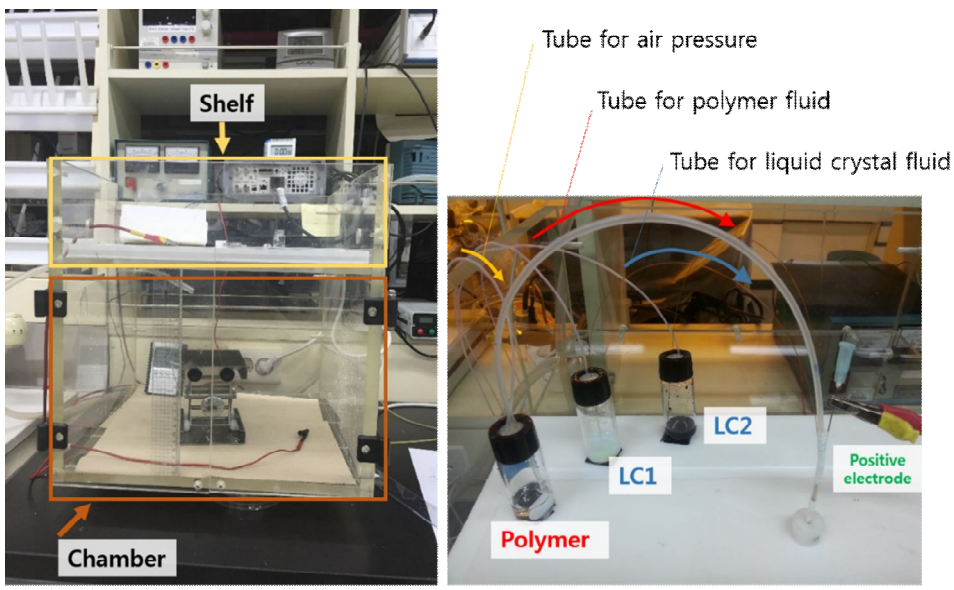

Figure 9. Electrospinning chamber and tube with silica capillary which connected with vials

Each of the vials containing the spinning fluids were connected with two tubes, one immersed into the fluid, the other ending in the air, just below the cap. The latter is connected to a Fluigent MFCS microfluidic control unit, which via this tube pressurizes the vial with a specific overpressure, set by the user in the control software. The overpressure then induces a flow of the spinning fluid through the other tube which ends in the spinneret, introducing the material to the Taylor cone and thus to the

jet. The flow rate was controlled by adjusting the overpressure in the relevant vial in the range of 10 mbar to 800 mbar. Because of the small volume of liquid crystal, we used thin flexible silica capillaries (BGB Analytic) for flowing core materials.

The high voltage driving the spinning was provided by a Gamma High Voltage power supply. A metal syringe needle was inserted into the tube carrying the polymer solution, and the hole thus produced was carefully sealed by Teflon tape, see right part of **Figure 9**. Now the positive voltage output of the power supply could be connected to the polymer solution by fixing an alligator clip to the syringe needle, with a cable running from the power supply to the clip. Another cable connected the ground electrode of the power supply to an aluminum foil which was used as collector.

3.2.2 Spinneret Design

The first design of the spinneret was composed of a plastic tube, two silica capillaries, a syringe needle and a glass capillary with theta shaped cross section, see **Figure 10**. The main plastic tube with outer diameter 3 mm and inner diameter 2 mm is directly connected to the vial for polymer solution and the other end is connected to the glass capillary with 2 mm outer diameter. The two silica capillaries, with 100 µm inner diameter, were inserted through holes made on each side of the plastic tube and guided into their respective channel of the theta shaped glass capillary. The metal needle was inserted into the main tube for applying the voltage to the solution.

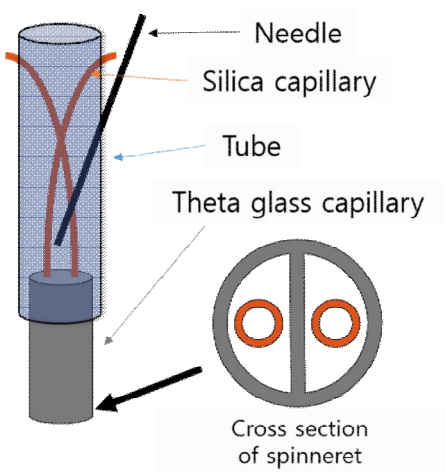

Figure 10. First spinneret design with tube, silica capillaries, theta shaped glass capillary and syringe needle for voltage application.

The configuration with flexible silica capillaries for the core fluids had the

disadvantage that it offers poor control of the positions of the capillary ends within the theta capillary. From one experiment to another, repeatability of the spinneret configuration was thus limited. We therefore designed a second generation spinneret where the silica capillaries for the core fluids were guided through 23G flat edge metal needles. This had the further advantage that the alligator clip from the power supply could be attached to these needles. The outer diameter of the needles was close to the maximum channel width of the theta capillary, giving them a fixed position in this capillary, see right side of **Figure 11**. The theta capillary was now fitted to one end of a piece of stiff plastic, having a branch off to the side close to its other end, see left side of **Figure 11**. The polymer solution was fed through the branch while the two needles extended through the main opening of the piece, via a rubber stopper that sealed off the tube.

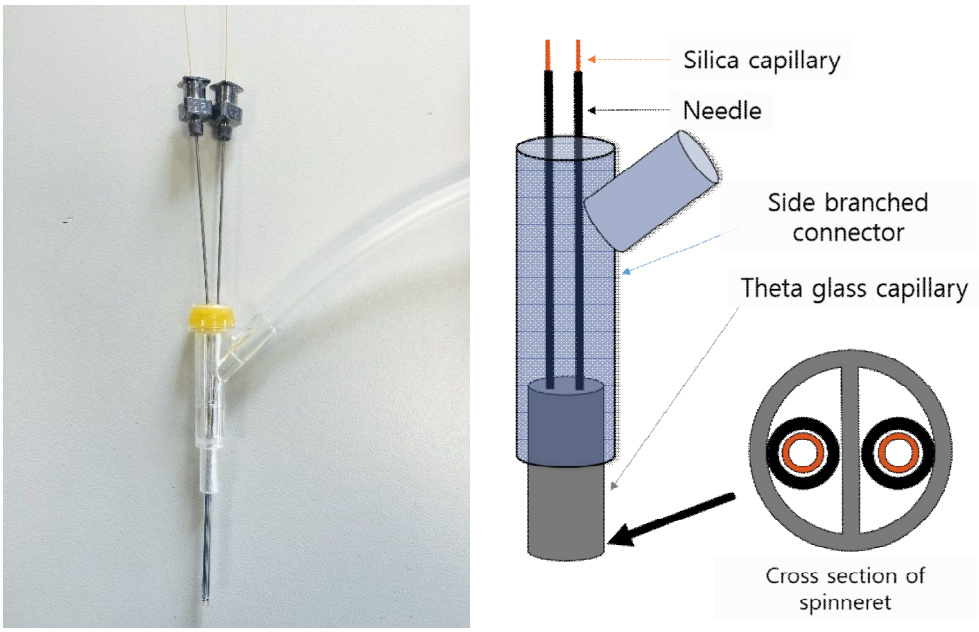

Figure 11. Picture of second generation spinneret, designed with side branched connector and two metal needles guiding the core fluid capillaries (left) and the sketch of the spinneret (right).

Two sizes of theta glass capillary were purchased commercially (Friedrich & Dimmock, Inc, USA), with 1.5 mm and 2 mm outer diameter, respectively. The corresponding inner diameters were 1.0 mm and 1.4 mm, and in both cases the septum (the wall separating the two channels) was 0.2 mm thick. The main benefit of using glass is the transparency, aiding in observing the spinning fluids, liquid crystal as well as polymer solution, in the spinneret. It also allows us to verify that the silica capillaries end at an appropriate height above the Taylor cone.

3.2.3 Calculating Flow Rates

Three different flexible silica capillaries were used in the experiments, with outer diameters 450 μm, 250 μm and 170 μm. The capillary diameter is very important because it greatly influences the flow rate as expressed by the 'Hagen-Poiseuille equation':

$$\Phi = \frac{dV}{dt} = v\pi R_i^{\,2} = \frac{\pi R^4}{8\eta}\frac{\Delta P}{L} \qquad (4)$$

Here Φ is the flow rate in volume per time (dV/dt) which in the cylindrical geometry of the capillary can be written in terms of the flow velocity v and the channel cross section area πR_i^2, where R_i is the inner radius of the capillary. The equation relates this flow rate to the pressure difference between the two ends (ΔP), the dynamic fluid viscosity (η) and the length of the capillary (L), allowing us to calculate the flow rate of materials at a given overpressure.

The MFCS is able to supply a stable overpressure ΔP from 20 mbar to 600 mbar. When we pump 5CB (η = 0.028 Pa·s) through 25 cm long silica capillaries of different diameters the achievable flow rate range can be calculated as summarized in table 1.

Table 1. Range of 5CB flow rate through the three types of flexible silica capillary used in the study, considering 25 cm capillary length.

R_i (μm)	ΔP (mbar)	Φ
100	20	0.002
	600	0.07
250	20	0.1
	600	0.10
340	20	0.33
	600	10.11

The cross section area of each channel of the glass theta capillary was calculated to match the conditions in the reference experiment by Li et al. [24]. In this paper a triple-core coaxial spinneret was used, where the main spinneret had outer diameter (OD) of 3.5 mm and inner diameter (ID) of 2.0 mm, and the three inner capillaries had OD 0.4 mm and ID 0.2 mm. With these data, we can calculate a target ratio of the available sheath solution cross section area to the total cross section area of the three core fluid flows, yielding the value 35:1. With our available flexible silica capillaries and theta glass capillaries, the following ratios were achievable in our experiments:

Table 2. Cross section ratio for sheath solution and core material for each combination of our capillaries.

Outer diameter of glass capillary (mm)	1.4			1		
Outer diameter of silica capillary (mm)	0.435	0.350	0.170	0.435	0.350	0.170
Ratio (sheath/2 inner core)	6.54	12.44	82.31	2.38	4.87	35

The closest match ratio with the reference data was obtained with the smallest silica capillary in the smallest theta capillary. However, with our choice of fluids a ratio higher than 35:1 turned out to be optimal and therefore most experiments were carried out with the smallest silica capillary in the larger theta capillary. The drawback of this solution was that rather viscous polymer solutions had to be used, since otherwise dripping occurred from a theta capillary this large. This required us to use relatively high polymer concentration as well as added $Ti(OiPr)_4$.

3.2.4 Monitoring of Taylor Cone

For successful production of dual core fibers it is important to monitor the quality of the Taylor cone during spinning. This was done by mounting a USB camera with appropriate objective close to the spinning chamber, such that a detailed image of the end of spinneret and the Taylor cone could be monitored on the computer screen.

According to a study of single core coaxial electrospinning by S.N Reznik et al., it is desirable if the inner capillary protrudes by a distance equal to half of the outer spinneret radius [25]. Such a large protrusion is impossible when having multiple core capillaries, since their position is closer to the edge of the Taylor cone. Therefore, we used the camera to aim for a core capillary positioning as low as possible without breaking the Taylor cone.

3.2.5 Polarizing Microscopy

All micrographs in the thesis, showing the optical characteristic of the liquid crystal and phase transitions in the fiber, were obtained using an optical microscope (Nikon Eclipse LV100 or Olympus BX51) as well as a heating system, Instec TS-62 or Linkam T95-PE hot stage.

3.2.6 Scanning Electron Microscopy

To observe the cross section of fibers, a Hitachi S 4800 field emission scanning electron microscope (FE-SEM) was used. The OTS hydrophobic treated substrate was used as the collector for the sample which could be inserted in the SEM after coating of the fibers with platinum (2 nm layer deposited). To see the cross section, the fiber had

been dried in air for a day after which it was cracked together with the substrate, prior to platinum coating. In order to obtain a clean cross section, complete drying was necessary and a good contact with the substrate is required.

3.2.6.1 Electrospinning Conditions

As described above, the fluids were pumped using the MFCS microfluidics control unit. The flow rate for polymer was in the range 0.004–1.1 ml/hr and for liquid crystals 0.07–0.09 ml/hr. The flow rate for each fluid is calculated from the applied pressure and capillary diameter and length through the Hagen-Poiseuille equation. The distance between the spinneret and collector was controlled between 9–11 cm and the supplied voltage was 9–12 kV.

4 Results and Discussion

4.1 Stable Spinning with Dual core

4.1.1 Monitoring of Taylor Cone and the Onset of Spinning

The key requirement for the successful production of dual core fibers is a stable separation of the two core materials. The septum of the glass capillary and the metal needles that guided the silica capillaries in the second generation spinneret helped to keep the core materials apart. However, if the balance in flow rate between the three flowing fluids is not appropriate, the core fluids may mix in the Taylor cone, and also the applied voltage has an important effect. Therefore, the characteristics of the Taylor cone were carefully monitored with a camera during all experiments.

At high flow rate of liquid crystals the core streams expand after exiting the silica capillary into the Taylor cone, where they then merge. The same thing happens if the flow rate of the polymer solution is too low (see **Figure 12** (b)). Also the voltage plays a role in determining the Taylor cone shape and monitoring the Taylor cone makes it easier to find the appropriate voltage to supply. For instance, at too low voltage, spinning fluid regularly separates as large droplets from the Taylor cone. If the

voltage is instead too high, multiple Taylor cones of reduced size were generated. The dye-doped liquid crystal was particularly easy to visualize within the Taylor cone, even at the point where the jet is spun out. This was therefore used in early experiments in order to establish an understanding of how the Taylor cone should appear for successful spinning. The monitoring of the process is further facilitated by the transparency of the glass capillary.

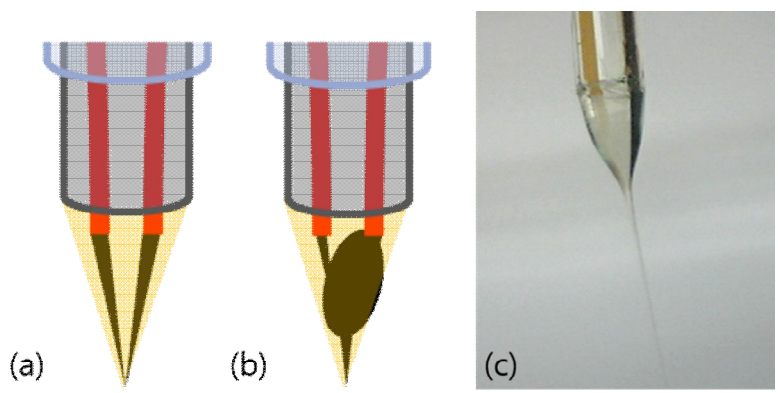

Figure 12. Sketch of Taylor cone with ideal liquid flow (a) and in an unbalanced state (b). The imbalance of polymer solution and core fluid leads to the core material forming a drop within the Taylor cone. This can result in dripping or mixing of the two liquid crystals into a single core. A photograph of an ideally shaped Taylor cone with two nematic liquid crystal cores (one of them is doped with a black dye) is shown in (c).

4.1.2 Counteracting Fiber Collapse after Collection on Target Substrate

While the black ROTN liquid crystal helped in observing the fluid of core material in the Taylor cone, the core thickness in the produced fiber was too low to distinguish the color from the dye. Therefore, both cores looked like regular nematics when studying the fibers in the optical microscope. To allow sufficient contrast between the cores also in the fiber, we therefore replaced the regular nematic core fluid with a short pitch chiral liquid crystal (ROTN and CB15) showing selective reflection of visible light. **Figure 13** shows a fiber where the red reflection color of the chiral liquid crystal mixture is easy to distinguish from the white nematic appearance of the dyed ROTN. This confirms that the two liquid crystals were well separated in the fiber. However, in locations where fibers crossed one can easily see that the fibers have merged, indicating that they were in a wet state at the time of the deposition. This wet state also had the effect that the fibers largely collapsed into a flattened shape rather than the expected cylindrical shape.

The reasons for fiber collapse and merging are too slow solvent evaporation or too high amount of core materials. When the fiber was deposited close to the spinneret, the jet did not have enough time in flight for sufficient evaporation, resulting in wet

fibers on the substrate. Moreover, the limited stretching did not allow for sufficient diameter reduction, hence the resulting fibers were rather thick. In the area where the fibers overlapped, they had merged and the inner material had been squeezed into droplets, as seen in **Figure 14**. The problem is related with the flying time in electrospinning. To increase the flying time of the jet, the distance between the capillary and collector can be extended, while the supplied voltage is increased in order to maintain constant electric field. Additionally, dry air is also helpful in accelerating the solidification of the fiber.

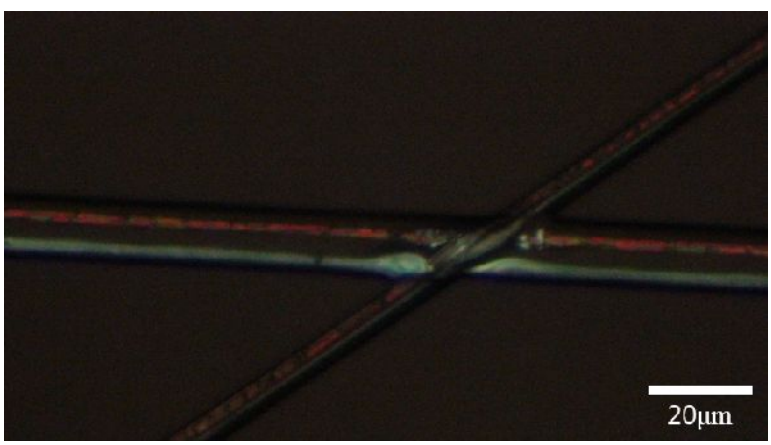

Figure 13. Reflection state of polarizing optic image. The flow rate of polymer solution was 0.4 ml/hr and 0.96 ml/hr for each liquid crystal. The distance between the spinneret and collector was 13 cm while the applied voltage was 10.5 kV. The fibers were deposited on a glass slide. The scale bar is 20 μm.

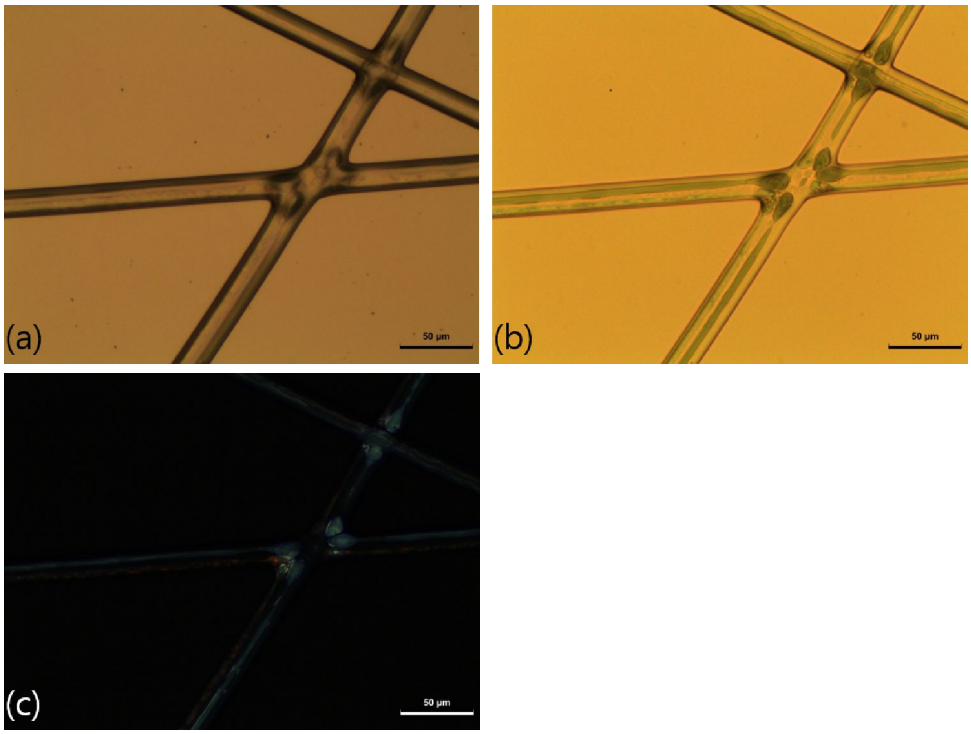

Figure 14. Optical microscopy images of fibers with dye-doped ROTN in one core and chiral nematic in the other, in reflection (a), transmission (b) and reflection with crossed polarizer (c). The flow rate of polymer solution was 0.4 ml/hr and 0.96–1.1 ml/hr for liquid crystals. Distance between the spinneret and collector was 11.5 cm while the supplied voltage was 7 kV. The sample is prepared on glass slide. The scale bar is 50 µm.

4.2 Two Cholesteric Liquid Crystals Encapsulated in the Same Fiber

The chiral liquid crystal mixture appeared with color in reflection with crossed polarizers, whereas the non chiral nematic liquid crystal is rather dark under this condition. This shows up more brightly in transmission between crossed polarizers. In order to achieve fibers with two cores that could easily be distinguished in the same microscopy mode, the next stage of the experiment was using two chiral liquid crystal mixtures with different pitch and thus different reflection colors. **Figure 15** shows reflection polarizing microscopy photos of some different fibers produced with these mixtures and it is clear that the two cores can be easily distinguished. However, it is also obvious that the color may change from one fiber to another, a result that is most likely due to the effect of confinement on the cholesteric pitch. [16].

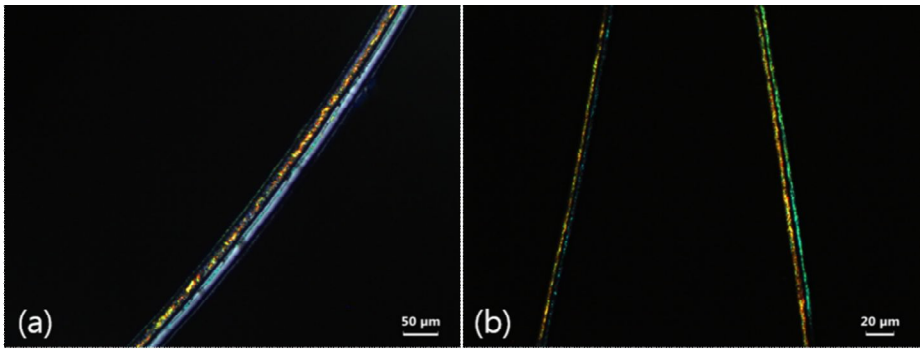

Figure 15. Two different cholesteric liquid crystal core fibers. (a) had 0.4 ml/hr for polymer solution flow rate, 10cm distance and 6 kV as supplied voltage while (b) had 0.8 ml/hr with 11.5 cm distance and 7 kV. both of (a) and (b) had 4.8 ml/hr for liquid crystal flow rate.

Both of the samples in **Figure 15** were spun with an electric field of 0.6 kV/cm, but with 1.5 cm longer spinneret-collector distance in (b). The flow rate of polymer was also increased in (b) in order to sustain the wall which separates the core materials despite the increased elongation. The difference in spinning parameters gave the sample in (a) a thickness of 30–35 µm, while the sample in **Figure 15** (b) is substantially thinner. Considering how this influences the color of the cores, as well as the fact that any mixing between the core fluids would also lead to color change, we then heated the fibers in order to investigate the clearing temperatures of each core, hoping that this would allow clear distinction between the core materials. The result of the experiment is show in **Figure 16**. Unfortunately, the difference of clearing point

between the two chiral nematic mixtures was so small that also this experiment did not yield conclusive results. We therefore concluded that a different combination of liquid crystals was necessary in order to verify that the two cores were intact at the end of the process.

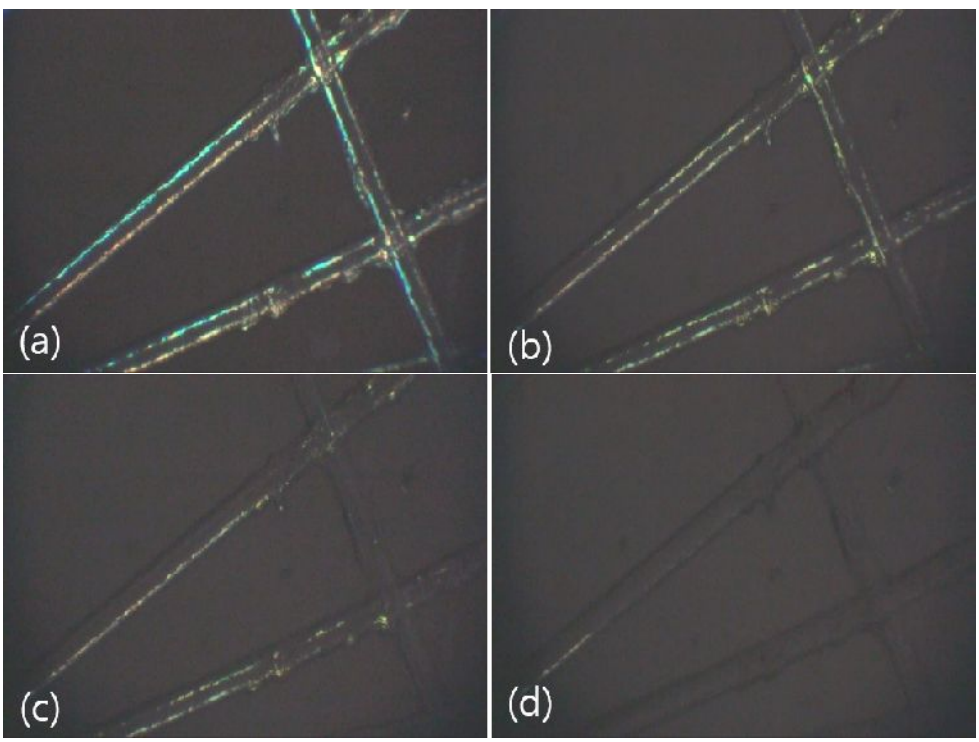

Figure 16. Heating experiment of fibers which were produced in a tapered glass capillary spinneret (340μm diameter opening). The flow rate for polymer was 0.004 ml/hr while the core material had 0.77 ml/hr (67:33) and 1.94 ml/hr (50:50). The distance was 9cm with supplying 6 kV voltage. The temperature is 20 ºC, 31 ºC, 33 ºC and 35 ºC in the sequence (a) to (d).

4.3 The Effect of Polymer Solution Concentration on the Inner Structure of the Fiber

To overcome the fiber merging problem, we explored the possibility of reducing the polymer concentration. Although this means we actually add solvent, the reduced elongational viscosity would allow greater stretching of the fibers in flight, thereby increasing the surface to volume ratio and thus allow a more complete evaporation of the solvent prior to deposition. Moreover, the diameter of the fiber should become lower. We decreased the polymer concentration from 18 wt% to 16 wt%, resulting in the fibers seen in **Figure 17**. The fiber is thinner and less collapsed, but the inner wall between the cores disappeared at the same time, resulting in single core fibers. Apparently, the separation between the cores could not resisted the increased stretching in the low concentration fibers.

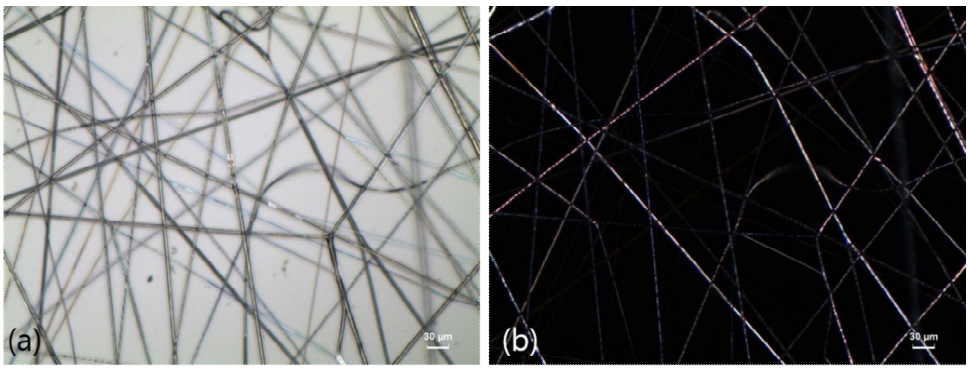

Figure 17. Optical microscopy pictures of fibers produced with 16 wt% PVP. The image in (a) was obtained in reflection without polarizers, and that in (b) was in transmission with the sample between crossed polarizers. The flow rate for the polymer solution was 13.7 ml/hr and for the liquid crystals it was 0.4 ml/hr for 5CB and 1.29 ml/hr for the mixture of ROTN and CB15 (65:35 ratio). The distance from spinneret to collector was 13 cm and the applied voltage was 14.5 kV.

In order to support the dual core internal structure, we therefore tried spinning fibers from solutions with even higher concentration of polymer, although this should increase the fiber thickness [26]. The resulting fibers (see **Figure 18**) indeed have dual core, as revealed in polarizing microscopy (image (a)). However, the image without polarizer reveals that the cores have been pushed to the edges of the fiber with a very broad wall between them. What has most likely happened is that the outer layer of the jet solidified early during the flight, while solvent still remains further inside, leading

to collapse into a “dog bone” shape [27], as illustrated in the sketch in figure 18(C). This effect is due to the fact that diffusion of solvent from the jet interior to the surface is much slower than the evaporation from the surface. The surface therefore solidifies into a skin while there is still plenty of solvent inside the fiber. As eventually also this solvent evaporates the skin cannot shrink to fit the reduced volume under maintained cylindrical shape, giving rise to the collapsed fiber morphology. Because this collapse process could have induced two separate cores even from a single mixed core, we cannot be certain that the materials in the two cores of the final fibers we are not intermixed. Hence, we made no further investigation with fibers of this type. The dog bone shaped fiber was also seen in fiber produced with titanium isopropoxide if the ethanol contained a small amount of water.

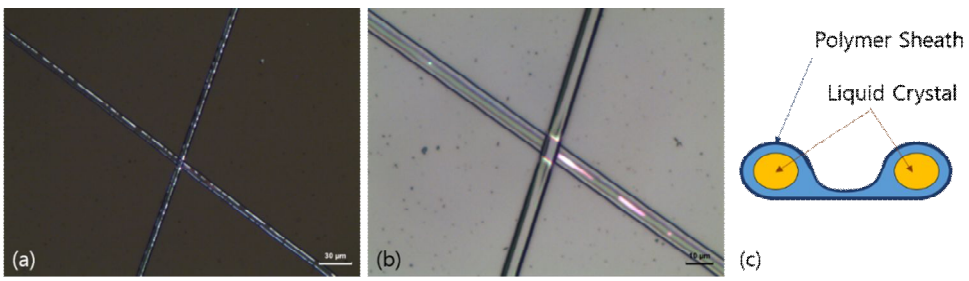

Figure 18. Fiber which produced with 20 wt% PVP. The picture (a) is the reflection with crossed polarization state, (b) is reflection without polarization and (c) is cross section sketch of dog bone shape fiber. The flow rate for polymer was 1.9ml/hr and for liquid

crystal were 0.04 ml/hr for E7 and 0.07 ml/hr for 5CB. Distance between the spinneret and collector was 6 cm and the supplied voltage is 8 kV.

4.4 Dual Core Fiber with Two Different Encapsulated Nematic Liquid Crystals

To test whether the dual core fiber is stable throughout the spinning process, we decided to spin fibers with two different nematic liquid crystals, 5CB and E7, with more than 20 ºC difference in clearing point (35.3 ºC for the single component nematic 5CB and about 60.5 ºC for E7). If the two cores remain intact and separated, it should be easy to distinguish the clearing points of the 5CB and E7 core, respectively, during a heating experiment. If the core fluid mix, however, then we may expect a single intermediate clearing point for both cores. The result of the first experiment, where the fibers were deposited on glass, is shown in **Figure 19**. Initially, the two cores appear different with significantly different colors, however, upon heating one core turns isotropic at about 40 ºC, and the other at about 45 ºC. This demonstrates that the two liquid crystals were mixed at some stage during fiber production, although some difference remained between the two cores. While the bulk liquid crystals have more than 20 ºC difference in clearing point, the liquid crystals in the fiber cores have a

small temperature difference, 3–5 ºC.

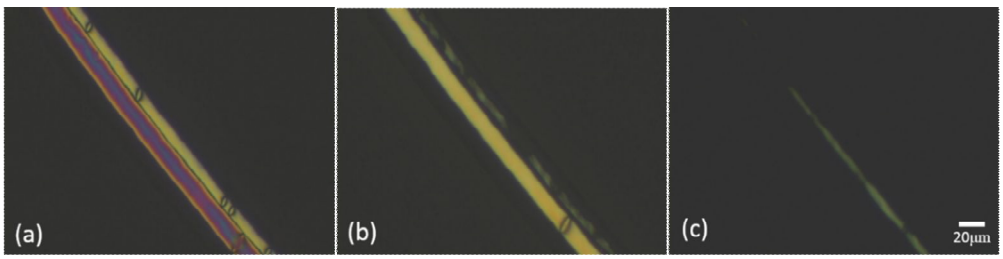

Figure 19. Fiber filled with E7 and 5CB observed in transmission between crossed polarizers. The fiber was prepared with flow rates: 0.8 ml/hr for polymer fluid, 0.13 ml/hr for E7 and 0.09 ml/hr for 5CB. The temperature was 25 ºC, 40 ºC and 45 ºC from left to right.

The separation between the cores was extremely fragile, as further confirmed by studying the texture of the fiber upon cooling. **Figure 20** shows the same fiber as in **Figure 19** after it was cooled down to room temperature. The unstable inner wall between the cores was apparently destroyed in the heating process, leaving a single thick core in which the liquid crystal exhibit a defect rich texture at room temperature.

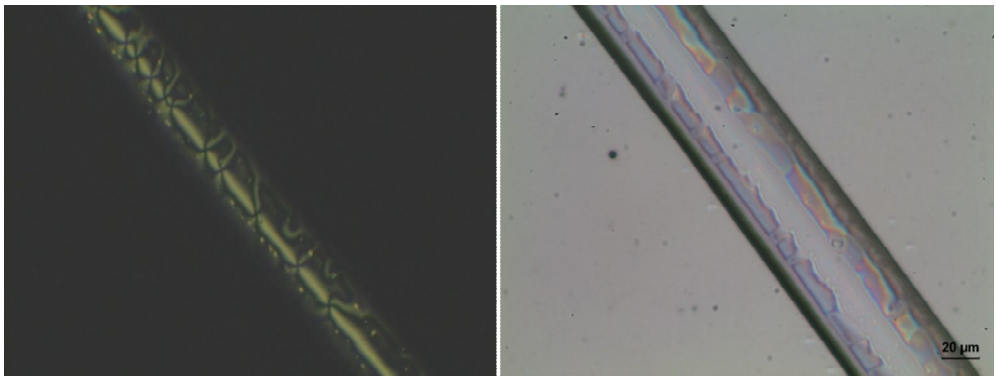

Figure 20. Cooled liquid crystal-filled fiber (same as in figure 19) after heating. Transmission state with polarizer (left) and reflection state (right) of the fiber.

Considering the observation by Kim and Lagerwall that capillary forces due to condensed water can have a drastic impact on core-sheath fibers when they are deposited on hydrophilic substrate[17], we now tested depositing the 5CB/E7 fibers on hydrophobic substrates instead. Indeed, fibers deposited on OTS treated substrates showed a stable separation of core materials and distinctly different clearing points of the two liquid crystals, although they were still different from the bulk transition temperatures, as discussed in the following.

Figure 21 shows two 5CB/E7 fibers deposited on a hydrophobic substrate. One is so thin that core mixing occurred in flight, but the other has well separated cores. The heating experiment of this fiber shows clearly different phase transition temperatures (see **Figure 22**). The fiber is heated from 20 ºC and the temperature increased 1 ºC per

minute. The first phase transition starts at 25 ºC and the adjacent core transforms into isotropic at 46 ºC. In contrast, the thinner fiber with mixed core shows only one clearing point at 40 ºC. On cooling, the phase transitions in each core occurred at about the same temperatures, confirming that the wall separating the cores in the thick fiber remained intact.

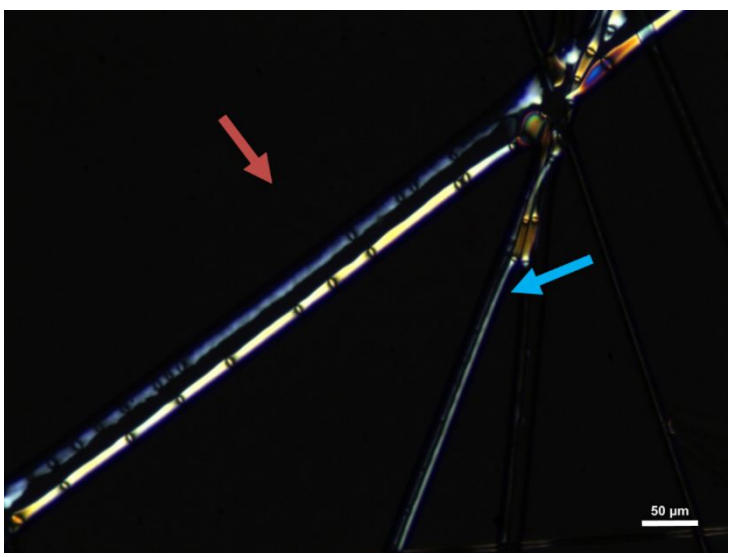

Figure 21. 5CB and E7 dual core fiber (red arrow) and mixed core fiber (blue arrow) deposited on hydrophobic substrate. The flow rate for polymer solution was 1.2 ml/hr and for liquid crystals were 0.07 ml/hr (5CB) and 0.05 ml/hr (E7). The distance between spinneret and collector was 8 cm and applied voltage was 10 kV.

Figure

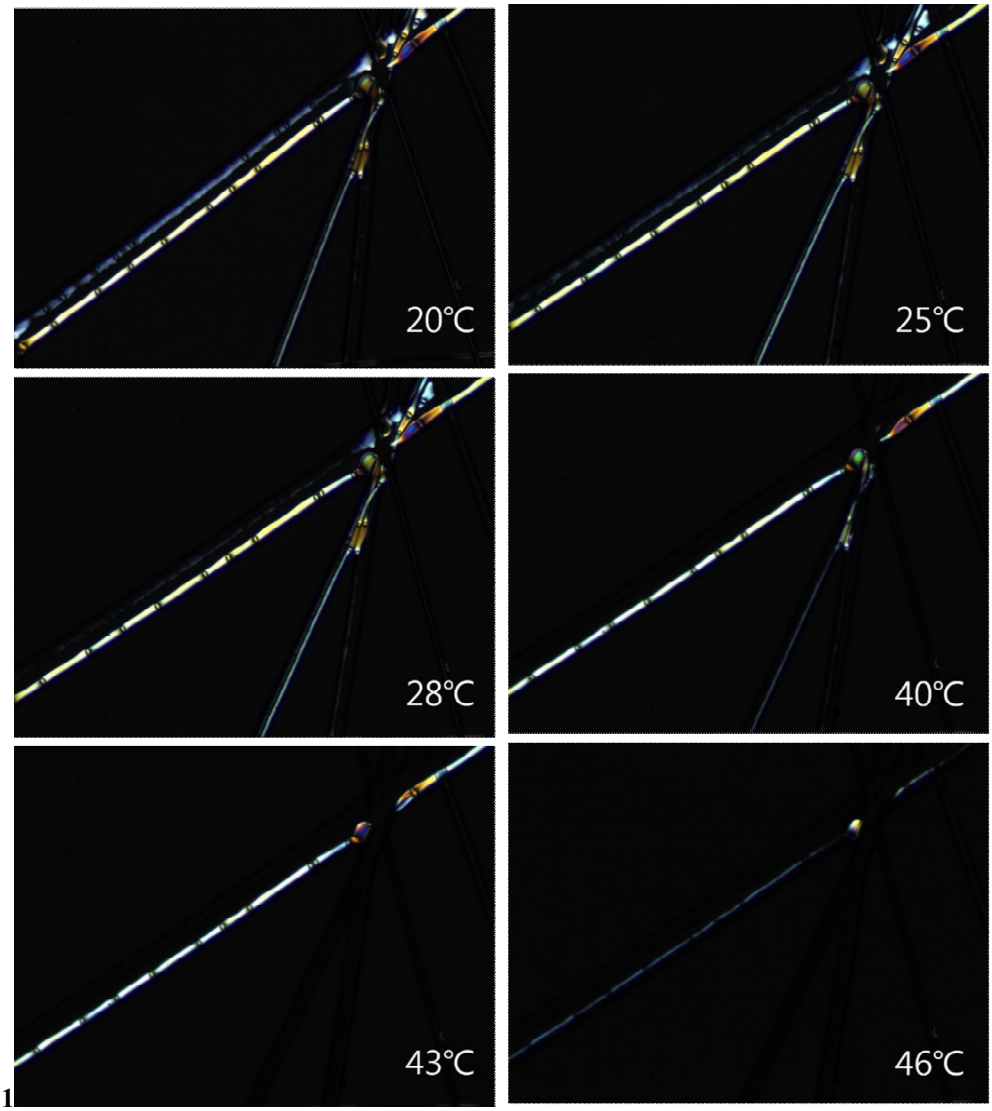

21

Figure 22. The fibers from figure 21 as they are heated until all cores have gone through the phase transition to the isotropic state. The heating process was from 20 ºC to 46 ºC with a heating rate of 1 ºC/min. While the thick fiber with well separated dual cores shows two distinct clearing points at 25 ºC and 46 ºC, the thinner mixed core fiber has only one at 40 ºC.

The use of hydrophobic substrates was thus successful in preventing post deposition mixing of the cores, but the clearing points in the two cores were still very different from the bulk transition temperatures. In both cores the clearing point was considerably lower than the respective bulk liquid crystal. The reason for this suppression of transition temperatures inside the fiber is presently not clear, but we may speculate about possible causes. Since *both* cores exhibited a decrease in clearing point the reason cannot be a simple mixing of the two core fluids, since that would have led to an intermediate clearing point, as in the thinner fiber in figure 21- 22. Next, one might suspect that the encapsulation inside the fibers would have affected the phase transitions. However, while such an effect can indeed be considerable, it always leads to an *increase* in transition temperature in the cylindrical confinement provided by the electrospun fibers [16] [28].

The most likely reason for the change in transition temperature is contamination of each LC core by a non-liquid crystalline material. In our case, such a contaminant would be expected to come from the polymer sheath solution, possibly with the addition of water that condenses on the fiber during spinning. Considering the composition of our sheath solution, the culprit is most likely the surfactant. We know that water condensed from the air enters the polymer solution during flight, as this is a prerequisite for the chemical reaction that turns $Ti(OiPr)_4$ into TiO_2. With surfactant

present in the polymer solution some of this water may migrate into the liquid crystal, hidden by an inverse micelle arrangement of surfactant molecules. This is particularly likely considering our rather high polymer concentration, which may lead to a skin of solid polymer forming on the outside of the jet while water is still inside. The much slower diffusion of water through the solid polymer skin makes it more likely that a water containing inverse micelle may find its way into the liquid crystal core. Such a scenario would indeed suppress the clearing point of the liquid crystal since the inverse micelle strongly disturbs the nematic order.

While further experiments would be needed to corroborate this explanation, two additional samples prepared within the scope of this thesis work provide evidence that the thick dual core fiber shown in Figure 21–22, deposited on hydrophobic substrate, indeed represents successful separation of the two core materials. **Figure 23** shows the heating experiments corresponding to that of Figure 22, but carried out on single core fibers, with 5CB and E7 in the core, respectively. The polymer solution was identical to that used for dual core spinning. Note that the clearing points in both cases are lower than in the pure bulk 5CB and E7, respectively. In fact, they are identical to those seen in the thick dual core fiber in Fig 21, suggesting that no mixing between the cores occurred when producing the latter fiber, and that the same contaminant—presumably water inside an inverse surfactant micelle—is present as in the single core fibers.

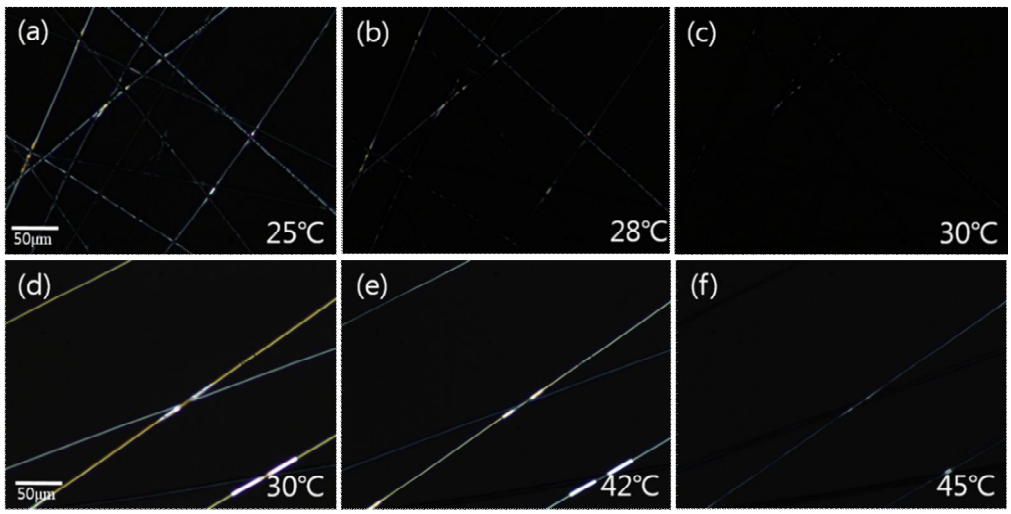

Figure 23. Single liquid crystal fiber with 5CB (a–c) and E7 (d–f). While the bulk state of 5CB had phase transition at 33 ºC, the fiber prepared in the fiber had it at lower temperature, 28 ºC. E7 also experienced clearing point shift from about 60 ºC to 45 ºC.

In order to get a nanoscale confirmation of the dual core fiber geometry we attempted to break fibers in such a way that the cross section can be imaged by SEM. This is not trivial since most breaking procedures will lead to a closing of the cross section as the sheath collapsed. We eventually found a route to success by depositing the fibers on a silicon chip which had been lightly scarred with a diamond knife at one edge. After drying the fibers at room temperature in ambient atmosphere for a day the chip with fibers was broken by applying pressure to the scar. This leads to a fast clean

cut along one silicon crystal direction, sometimes breaking also fibers that cross the path of the cut so fast that the cross section remained intact. The sample was coated with platinum and then studied by SEM. In many cases the cross section was difficult to resolve but in one case an excellent view of the two cores emerged, as seen in **Figure 24**. The two holes clearly visible in these images constitute the cores which prior to vacuum suction was filled with liquid crystals.

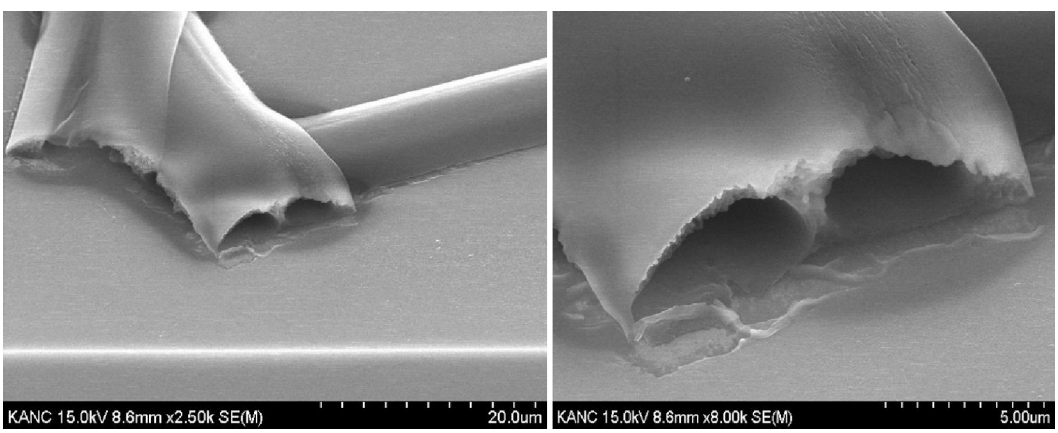

Figure 24. SEM images of cross section of a fractured dual core fiber spun with 5CB and E7, respectively, as core fluids, deposited on an OTS treated silicon substrate.

5 Conclusion

In this thesis, the production of dual core fibers with two different encapsulated liquid crystals has been introduced. To ensure stable and separated cores in the fibers, the materials, electrospinning setup (spinneret, collector and the condition of electrospinning like distance and voltage) had to be optimized carefully. By monitoring all stages of the spinning process, from the first meeting of the different fluids in the composited Taylor cone to the characterization of the final fibers on the target substrate, we could get a conclusive picture of how different parameters influence the results.

The main conclusions can be summarized as follows:

- Continuous monitoring of the Taylor cone is essential for success, because deviations from the ideal cone shape promotes core fluid mixing and may lead to poor fiber morphology.

- A high concentration of sheath polymer is needed in order to ensure a stable wall between the cores.

- A convenient choice of core fluids for verifying the quality of dual core geometry is nematics with clearing points that differ by at least 10–20 ºC. A simple heating experiment in the polarizing microscope can then verify whether or not the two

cores are well separated.

- The fibers should be collected on a hydrophobic substrates to avoid deformation due to capillary forces from water that spreads from the fiber across the substrate, promoting a mixing of the cores after deposition.

- The surfactant in the polymer sheath solution - added in order to increase conductivity and decrease surface tension, thus stabilize the electrospinning process - turns out to give an unexpected (and generally undesired) effect in the liquid crystal core. Because water condenses on the fiber during spinning, and then mixes into the polymer sheath solution, the surfactant can migrate together with water into the liquid crystal core, forming reverse micelles that strongly decrease the nematic phase stability.

6 Reference

1. D.K, Kim et al., J. phys. Chem.B., 2013 **51**(11), 855-867.
2. Yong Zhao et al., J. Am. Chem. Soc., 2007 (129), 764-765.
3. Wang, N et al., Macromol. Rapid Commun, 2010. **31**(18), 1622-1627.
4. H, Chen et al., Langmuir, 2010. **26**(13), 11291-11296.
5. J. P. F. Lagerwall, and G. Scalia, Current Applied Physics, 2012, 12, 1387-1412
6. D. Demus et al., Handbook of Liquid Crystals, volume 1-3, Wiley-VCH Verlag, Weinheim, 1998
7. P,Palffy-Muhoray., Nature, 1998. **391**.745-745
8. M. Bognitzki et al., Adv. Mater, 2001. **13**(1), 70-72.
9. D, Li et al., Nano Letters, 2004. **4**(5), 933-938.
10. H, Jiang et al., J Control Release, 2005. **108,** 237-243.
11. D.G, Yu et al., Mater. Lett, 2012. **67**(1), 78-80.
12. H, Yang, et al., ACS Nano. **6** (1): p. 622–628.
13. S.G,Taylor, Proc. R. Soc. Lond. A, 1964. **280**(1382), 383-397.
14. C, Burger et al., Annu. Rev. Mater. Res, 2006. **36**(1), 333-368.
15. J.T, McCann et al., Nano Lett, 2006. **6**(12), 2868-2872.
16. E, Enz and J.P.F Lagerwall, J. Mat. Chem, 2010. **20**(33), 6866-2672.
17. D.K. Kim and J.P.F Lagerwall, ACS. Appl. Mater. Interfaces, 2014. **6**(18), 16441-16447.
18. D. A.H. Hanaor et al., Adv. Appl. Ceram, 2012. **111**(3), 149-158.
19. D.P, Birnie, J. Mater. Sci, 2000. **35,** 367– 374.

20. C.K, Saner et al., Beilstein J Nanotechnol, 2012. **3**, 114-122.

21. Y.W. Yi et al., J. Appl. Phys, 2008. **104** (023534).

22. D, Li and Y. Adv. Mater, 2004. **16**(14), 1151-1170.

23. S.D, Vrieze et al, J. Mater. Sci, 2009. **44**(5), 1357-1362.

24. F, Li et al., *Nanofibers*, ed. A. Kumar. 2010: InTeck. ISBN 978-953-7619-86-2

25. S.N, Reznik et al., Phys. Fluids, 2006. **18**(6), 062101.

26. W.K, Son et al., Polymer, 2004. **45**(9), 2959-2966.

27. S,Koombhongse et al., J. Polym. Sci. Pol. Phys, 2001. **39,** 2598–2606.

28. J.P. Lagerwall et al., Chem. Commun , 2008(42), 5420-2.

요약 (국문초록)

전기 방사로 불리는 elecrospinning은 효율적이며, 저렴한 비용으로 1차원 나노구조소재를 구현하는 실용적인 방법으로 사용되고 있다. 더 발전된 기술로 coaxial electospinning은 spinneret에 추가적인 관을 삽입하여 섬유 안에 방사할 수 없는 물질을 넣어, 섬유에 새로운 물질의 성질을 더해 줄 수 있다. Liquid crystal은 고분자의 성질을 가지고 있지 않아 직접 방사가 불가능하지만, 고분자 피막 안에 넣음으로써 liquid crystal의 복굴절과 상변화 성격을 가진 섬유를 만들었으며 이 특성을 이용하여 유기물질의 유무를 알 수 있는 탐지기로의 기능을 가지도록 하였다.

본 연구는 Yong Zhao연구원의 coaxial electrospinning을 이용한 multichannel fiber를 바탕으로 섬유에 두 가지 다른 liquid crystal을 넣음으로써 1개 이상의 기능을 부여하고자 하였다. 기존 직접 제작한 spinneret 안 capillary가 표면장력에 의해 달라붙는 문제를 theta 모양의 유리관을 이용하여 해결하고자 하였으며, 유속, 거리, 전압, 습도 등의 요소 조절을 통하여 보다 효율적인 dual core fiber를 제작하였다. 더 나아가 collector의 hydrophobic과 hydrophilic 성격이 fiber의 내부구조에 영향을 줄 수 있는 연구 결과를 이용하여 보다 안정적인 dual core fiber를 생산하였다. 섬유 안의 liquid crystal은 내부구조의 안정성을 확인하는 지침이 된다. Liquid crystal의 복굴절 현상은 crossed polarizer 상태에서

고유의 색을 가지게 하여 섬유의 내부 구조를 시각적으로 확인 할 수 있게 되었다. 뿐만 아니라, liquid crystal 고유의 clearing point는 두 물질이 섞였을 때 그 온도가 평균화 되는 특성을 통해 섬유에 열을 가하는 방식으로 섬유의 내부 구조의 안정성을 확인 할 수 있다.

본 연구에서 개발한 방법으로 coaxial electroslinning을 두 개의 물질이 안정적으로 분리된, 기능성 섬유를 개발하였다. 이를 통해 섬유 안에 다수의 물질을 넣을 수 있음을 확인하였고, 보다 더 다양한 섬유의 기능을 넓힐 수 있을 뿐 아니라 넓게는wearable technology의 더 큰 가능성을 확인하였다.

.....

주요어 : 액정, 전기방사, 기능성 섬유,

학 번 : 2013-22393